SLAC–PUB–8565
August 2000

Plasma Focusing of High Energy Density Electron and Positron Beams *

J.S.T. Ng[1], P. Chen[1], H.A. Baldis[2], P. Bolton[2], D. Cline[3], W. Craddock[1], C. Crawford[4], F.J. Decker[1], R.C. Field[1], Y. Fukui[3], V. Kumar[3], M.J. Hogan[1], R. Iverson[1], F. King[1], R.E. Kirby[1], T. Kotseroglou[1], K. Nakajima[5], R. Noble[4], A. Ogata[6], P. Raimondi[1], D. Walz[1], A.W. Weidemann[7]

[1] *Stanford Linear Accelerator Center, Stanford, California, 94309*
[2] *Lawrence Livermore National Laboratory, Livermore, California, 94551*
[3] *University of California, Los Angeles, California, 90024*
[4] *Fermi National Accelerator Laboratory, Batavia, Illinois, 60510*
[5] *High Energy Accelerator Research Organization, Tsukuba, Ibaraki 305-0801*
[6] *Hiroshima University, Kagamiyama, Higashi-Hiroshima 739-8526*
[7] *University of Tennessee, Knoxville, Tennessee, 37996*

Abstract

We present results from the SLAC E-150 experiment on plasma focusing of high energy density electron and, for the first time, positron beams. We also present results on plasma lens-induced synchrotron radiation, longitudinal dynamics of plasma focusing, and laser- and beam-plasma interactions.

Invited talk presented at The 9th Workshop on Advanced Accelerator Concepts.
Santa Fe, New Mexico, USA
June 11-16, 2000

*This work was supported in part by the Department of Energy under contracts DE-AC02-76CH03000, DE-AC03-76SF00515, DE-FG03-92ER40695, DE-FG05-91ER40627, and the Univ. of California Lawrence Livermore National Laboratory, through the Institute for Laser Science and Applications, under contract No. W-7405-Eng-48; and by the US-Japan Program for Cooperation in High Energy Physics.

Table 1: FFTB electron and positron beam parameters for this experiment.

Parameter	Value	Units
Bunch intensity	1.5×10^{10}	particles per pulse
Beam size	5 to 8 (X), 3 to 5 (Y)	μm
Bunch length	0.7	mm
Beam energy	29	GeV
Normalized emittance	3 to 5 $\times 10^{-5}$ (X), 0.3 to 0.6 $\times 10^{-5}$ (Y)	m-rad
Beam density	$\sim 7 \times 10^{16}$	cm^{-3}

1 Introduction

The plasma lens was proposed as a final focusing mechanism to achieve high luminosity for linear colliders [1]. Previous experiments to test this concept had been carried out with low energy density electron beams [2]. The goals of the SLAC E-150 experiment are to study plasma focusing for high energy, high density particle beams in the regime relevant to linear colliders, to obtain better understanding of beam-plasma interactions, and to bench-mark computer codes for plasma lens designs. Such studies will help to develop compact and economical plasma lens designs suitable for collider experiments. In this paper, we present preliminary results obtained recently by the E-150 collaboration on plasma focusing of high energy density electron and positron beams.

2 Experimental setup

The experiment was carried out at the SLAC Final Focus Test Beam facility [3]. The experiment operated parasitically with the PEP-II B-factory; the high energy electron and positron beams were delivered to the FFTB at 1 - 10 Hz from the SLAC linac. The beam parameters are summarized in Table 1.

A layout of the beam line is shown in Figure 1. The beam size was measured using a wire scanner system. A carbon fiber 4 μm or 7 μm in diameter was placed downstream of the plasma lens, adjustable along the beam axis in a range of 8 to 30 mm from the center of the lens. The Bremsstrahlung photons were detected in a Cherenkov type detector located 35 m downstream of the lens. The variation in photon yield as the beam scans across the wire provided a measure of the transverse beam profile from which the beam size was determined. A set of ionization chambers interleaved with polyethylene blocks, located 33 m downstream of the lens, was used to monitor the synchrotron radiation emitted as a result of the strong deflection of the beam particles by the plasma lens. This detector provided an independent measure of the focusing strength. A streak camera, monitoring the Cherenkov radiation from an aerogel target installed in the electron beam line downstream, was used to measure the longitudinal plasma focusing dynamics.

To create the plasma lens, a short burst (800 μs duration) of neutral nitrogen or hydrogen gas, injected into the plasma chamber by a fast-pulsing nozzle, was ionized by a laser and/or the high energy beam. The solenoid valve operated at 0.5 - 2 Hz. Its 0.8 mm orifice was

matched to a parabolic-shaped nozzle 5 mm long with an opening of 3 mm diameter. The transverse profile of the gas jet was obtained by scanning the high energy beam perpendicular to its axis. The gas jet diameter which determines the plasma lens thickness was found to be 3 mm over a distance of 1.4 to 3.4 mm from the nozzle exit. The neutral density was determined by interferometry to be 4×10^{18} cm^{-3} for N_2 and 5×10^{18} cm^{-3} for H_2 at a plenum pressure of 1000 psi. The injected gas was evacuated by a differential pumping system which made possible operation of the gas jet while maintaining ultra-high vacuum in the beam lines on either side of the chamber. A schematic drawing of the plasma chamber is shown in Figure 2.

3 Results

The results presented below were obtained from data taken during the Fall of 1999 with electron beams and during the Spring of 2000 with positron beams. Measurements related to plasma focusing are presented first, followed by results on longitudinal focusing dynamics and laser- and beam-plasma interactions.

3.1 Plasma focusing

For a bunched relativistic beam traveling in vacuum, the Lorentz force induced by the collective electric and magnetic fields is nearly cancelled allowing it to propagate over kilometers without significant increase in its emittance. In response to the wakefield excited by the intruding beam, the initially uniform plasma electron distribution is perturbed in such a way as to neutralize the space charge of the beam and thereby cancel its radial electric field. For a positron beam, the plasma electrons are attracted into the beam volume thus neutralizing it; for an electron beam, the plasma electrons are expelled from the beam volume, leaving behind the less mobile positive ions which neutralize the beam. When the beam radius is much smaller than the plasma wavelength, the neutralization of the intruding beam current by the plasma return current is ineffective because of the small skin depth. This leaves the azimuthal magnetic field unbalanced which then "pinches" the beam, resulting in focusing. In this experiment, typical plasma densities are of the order of 10^{18} cm^{-3}, corresponding to a plasma wavelength of $\sim$30 μm which is indeed much larger than the incoming beam radius.

3.1.1 Beam self-ionization plasma focusing

A small fraction of the neutral gas molecules was ionized due to collisions with high energy beam particles. The secondary electrons from this impact ionization process were accelerated by the intense collective field in the beam, transverse to the direction of propagation, to further ionize the gas [4]. This beam self-ionization plasma was observed to focus the beam. That is, the head of the bunch was able to ionize the gas while the core and the tail of the bunch were focused. A more quantitative understanding requires detailed calculations which are not yet available for this experimental setup. The results for electron beams are shown in Figure 3. The wire scanner data were taken with the gas nozzle turned on and off at

each beam position, as the beam scanned across the wire, so as to minimize the systematics due to changes in beam conditions when comparing beam sizes measured with and without plasma focusing. The beam envelope was measured by changing the downstream position of the wire scanner; a reduction by a factor two in the transverse beam spot area was observed.

The beam self-ionization efficiency was determined for nitrogen gas by comparing the plasma focusing effects in two data samples. One sample was taken with the plenum pressure at 220 psi with beam self-ionization and also ionization by a Terawatt laser; while the other sample at 550 psi was taken with beam self-ionization only. Based on the laser performance and optical field ionization data [5], the Terawatt laser's ionization efficiency was estimated to be 10%. The beam size reduction was observed to be the same for the two data samples at one location along the beam waist. Assuming the plasma densities to be the same in both data sets, we arrived at a beam ionization efficiency of 7%. Note that this argument is only valid for low ionization yields.

3.1.2 Laser avalanche ionization plasma focusing

The results on laser pre-ionization plasma focusing presented here were obtained using a turn-key infrared laser system. It delivered 1.5 Joules of energy per pulse of 10 ns FWHM while operating at 10 Hz at a wavelength of 1064 nm. The laser light was brought to a line focus at the gas jet; the plasma thus produced was approximately 0.5 mm thick as seen by the e^+/e^- beams.

With the relatively long infrared laser pulse, the pulse front was able to ionize a small fraction of the gas by multiple-photon absorption; the resulting secondary electrons were accelerated, transverse to the laser's incident direction, to further ionize the gas resulting in an avalanche growth in plasma density. This growth is similar to the beam self-ionization process discussed in the previous section. The ionization efficiency was determined by interferometry to be 45% in this case.

The results for laser (and beam) ionization plasma focusing of positron beams are shown in Figure 4. The measured transverse beam size is shown as a function of the distance (Z) between the plasma lens and the wire scanner along the beam axis; the convergence of the beam envelope towards a waist can be seen. The first plot shows the focusing for nitrogen gas at 800 psi, while the second shows the result for hydrogen gas at 1100 psi plenum pressure. A reduction in transverse beam size by a factor of two is observed with laser (and beam) induced ionization; focusing is also observed with beam-induced ionization alone.

3.1.3 Synchrotron radiation induced by plasma focusing

The synchrotron radiation induced by the strong deflection of beam particles inside the plasma lens provides an independent measure of the plasma focusing strength. It also provides a pulse by pulse diagnostic of the transient plasma lens effect. The critical energy of the emitted synchrotron radiation scales with the strength of the focusing; a monitor was designed to measure the penetration profile, which depends on the energy spectrum of the photon flux.

The photon flux detected in the synchrotron radiation monitor contained various background contributions. There was Bremsstrahlung radiation accompanying the beam due to off-axis beam particles interacting with the vacuum chamber wall or upstream collimators, and also synchrotron radiation (with a critical energy ~250 keV) emitted when the spent beam was deflected towards the dump. This was measured with the gas jet turned off and the wire scanner removed from the beam. The contribution from beam-gas Bremsstrahlung, with the gas nozzle turned on, was determined by first measuring the Bremsstrahlung penetration profile from the carbon wire alone, then scaling this profile to the signal measured in the last depth section of the monitor with the beam-associated background removed. After these background contributions were subtracted, an excess in the photon signal beyond a depth of 3 radiation lengths was observed in the electron beam self-ionization plasma focusing data, for nitrogen gas at 550 psi plenum pressure. This excess was not observed when plasma focusing was weak (as determined from beam spot size measurements) for the case of lowered plenum pressure (to below 100 psi, for example), or for the case of hydrogen gas for which beam self-ionization was much less effective.

The penetration profile of the observed signal is consistent with synchrotron radiation with a critical energy of a few MeV according to Monte Carlo simulation. This value corresponds to a focusing gradient of the order of 10^6 T/m, as expected for the plasma lens parameters in this experiment.

3.2 Longitudinal focusing dynamics

A streak camera with pico-second time resolution was used to probe the variation in plasma focusing along the bunch. The Cherenkov light emitted as the beam passes through an aerogel target was imaged onto the streak camera. The vertical dimension of the beam was then measured in pico-second time slices along the bunch. The phase advance of the beam transport was such that focusing at the plasma lens becomes defocusing at the aerogel target. Therefore a larger beam spot at the Cherenkov target was expected because of the increased beam divergence due to plasma focusing.

The results from data taken with positron beams are shown in Figure 5, for nitrogen gas at two different pressures with beam self-ionization. The beam spot size in the vertical plane was measured with the gas nozzle turned on and off, and the difference is shown for time slices along the bunch. As expected, plasma focusing is significantly stronger at the longitudinal beam centroid. A detailed explanation of this result requires modeling of the beam self-ionization process which is currently under study.

3.3 Laser- and beam-plasma interactions

The laser avalanche ionization process has a finite build-up and decay time. By varying the laser pre-ionization timing before beam arrival at the plasma, different plasma densities can be probed by the high energy beam. The signal in the synchrotron radiation monitor is measured as a function of this advanced timing. Since this signal is predominantly synchrotron radiation induced by plasma lens focusing, the interaction between the high energy beam

and the plasma at various stages of formation and decay is monitored. This also means that focusing is observed well into the "after-glow" regime of the laser-induced plasma.

The result for positron beams and nitrogen gas at 1050 psi is shown in Figure 6. Time zero corresponds to coincidence between the beam arrival time and the peak of the recombination signal detected in a photomultiplier. The ionization efficiency is measured at time zero also. The synchrotron radiation monitor signal from beam self-ionization plasma focusing is 300 counts (as measured with the laser turned off); the beam-only background signal level is 80 counts (as measured with the gas nozzle turned off).

A quantitative understanding of this delay curve requires detailed modeling of the laser- and beam-plasma interaction process, as well as gas dynamics. A qualitative explanation of this curve is given here. The initial rapid increase in synchrotron radiation monitor signal most likely is due to an increase in plasma focusing strength, peaking at 500 ns. The data shown in Figure 4 are collected with this time delay, when the plasma density has decayed to an optimal level with respect to the beam density. The rapid rise is followed by a sharp decrease to the background signal level of 80 counts. This is predominantly due to an almost complete expulsion of the neutral and ionized gas volume driven by a laser-induced shock wave. Each gas jet pulse, lasting more than 100 μs, supplied a continuous stream of neutral gas molecules into the vacuum chamber at sonic speed. Therefore, this abrupt reduction is also assisted by the motion of the plasma, and by its decay. The remainder of the curve starting at 1.5 μs shows a diffusion driven gas recovery phase. Initially, the gas rushed back to fill the void, giving rise to an increased gas density locally above ambient level at 8 μs. During this time, we observe a corresponding rise in beam-ionization plasma focusing signal, on a slow time scale determined by gas dynamics. This is followed by a decay back to local equilibrium level of 300 counts within the time interval 8 to 12 μs. Additional data have been collected since the Workshop, with varying plenum pressures for nitrogen and hydrogen gases. A detailed simulation study should provide further insight into this delay-correlated modulation of plasma focusing.

4 SUMMARY AND OUTLOOK

Results on plasma focusing of 29 GeV electron and, for the first time, positron beams have been presented. Beam self-ionization turned out to be an economical method for producing a plasma lens; reduction by a factor of two in the beam spot area was observed with this method. The plasma focusing strength was also measured independently by monitoring the synchrotron radiation emitted by particles focused by the lens. The infrared laser with a 10 ns long pulse also proved to be efficient in plasma production, resulting in the strong focusing of positron beams. The longitudinal focusing dynamics was diagnosed with a streak camera with pico-second time resolution and, as expected, the focusing was strongest at the longitudinal center of the bunch. The laser- and beam-plasma interaction was studied by varying the laser pre-ionization timing with respect to the beam arrival time; we observed a delay-correlated modulation of the plasma focusing in the "after-glow" regime.

Design studies for linear collider applications are just starting. The first issue to resolve is the effect of beam jitter on the achievable luminosity of plasma focused beams. Plasma lens

parameters will also need to be optimized, which requires bench-marking of computer codes, as well as better understanding of the various plasma production processes. The experience gained in this experiment will serve as a basis for further engineering design studies for an eventual plasma lens application.

References

[1] P. Chen, Part. Accel., **20**, 171(1987).

[2] J.B. Rosenzweig *et al.*, Phys. Fluids B **2**, 1376(1990); H. Nakanishi *et al.*, Phys. Rev. Lett, **66**, 1870(1991); G. Hairapetian *et al.*, Phys. Rev. Lett. **72**, 2403(1994); R. Govil *et al.*, Phys. Rev. Lett. **83**, 3202(1999).

[3] V. Balakin *et al.*, Phys. Rev. Lett. **74**, 2479(1995).

[4] R.J. Briggs and S. Yu, LLNL Report UCID-19399, May 1982 (unpublished).

[5] B. Chang *et al.*, Phys. Rev. A **47**, No. 5, 4193(1993).

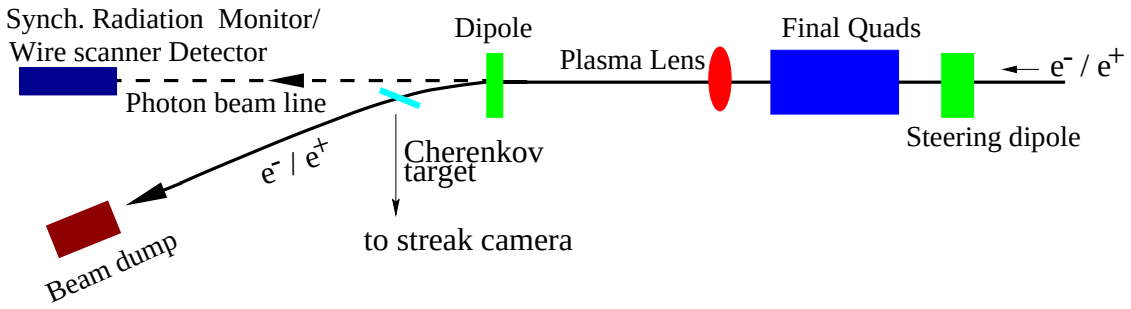

Figure 1: Layout of the plasma lens measurement setup.

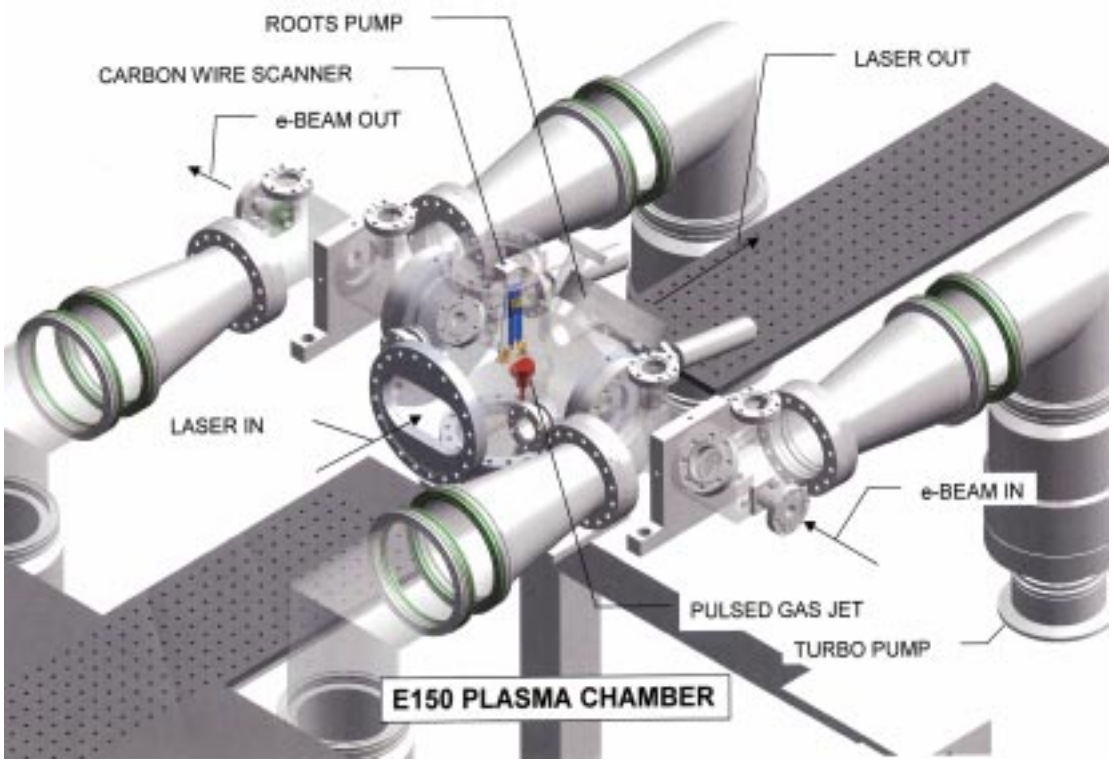

Figure 2: E-150 plasma chamber and differential pumping section.

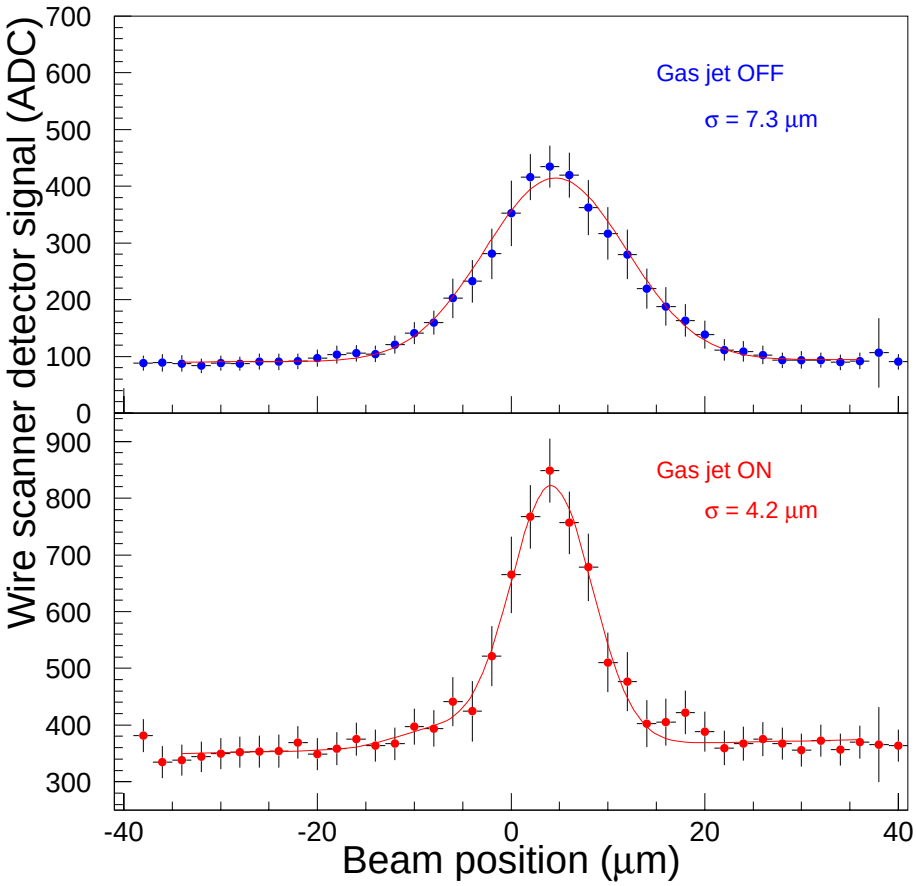

Figure 3: Wire scanner data showing focusing by a beam self-ionization plasma.

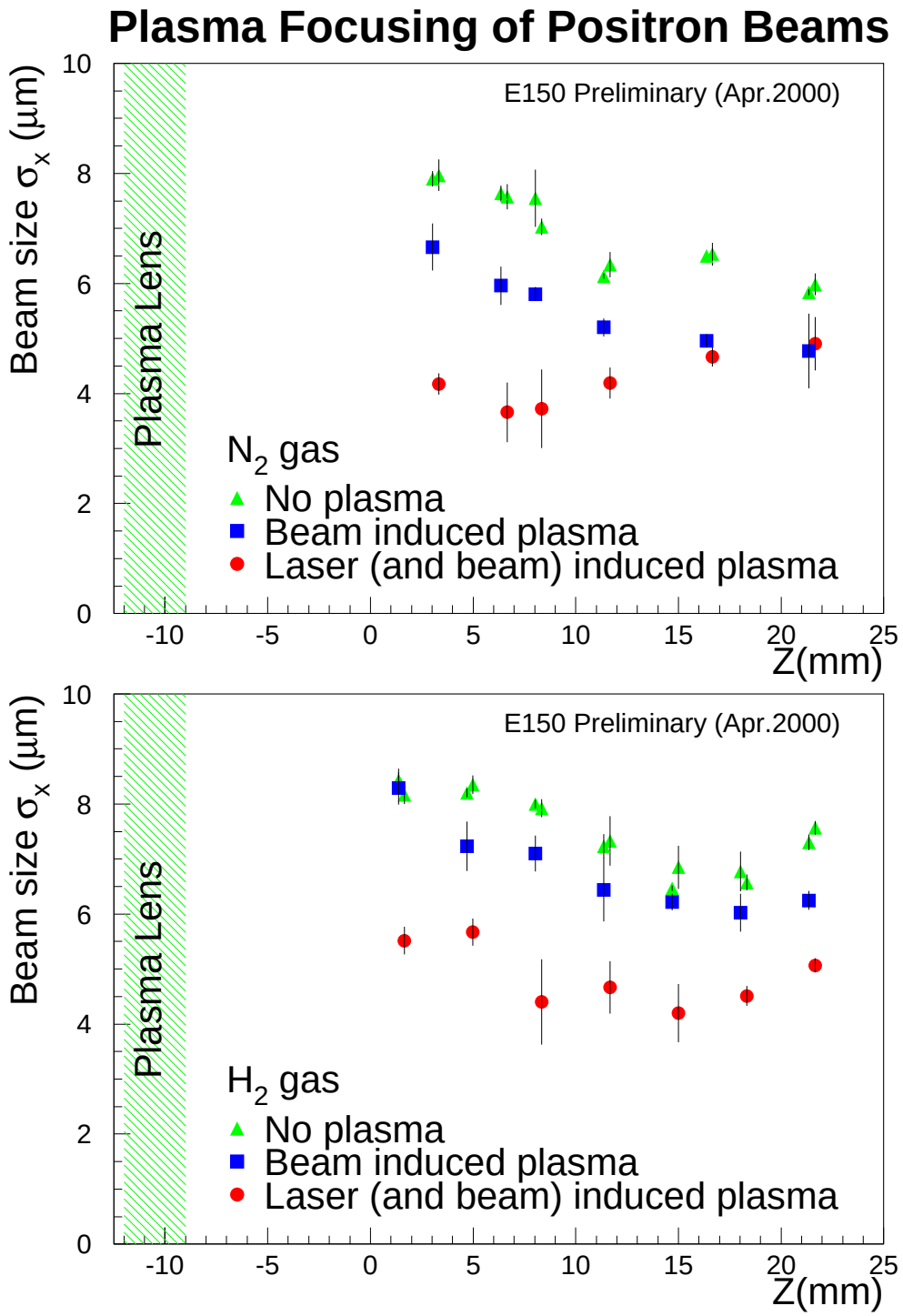

Figure 4: Evolution of the beam envelope, with and without plasma focusing, downstream of the plasma lens exit for two types of gases. The axis of the gas jet is at Z = -10.5 mm.

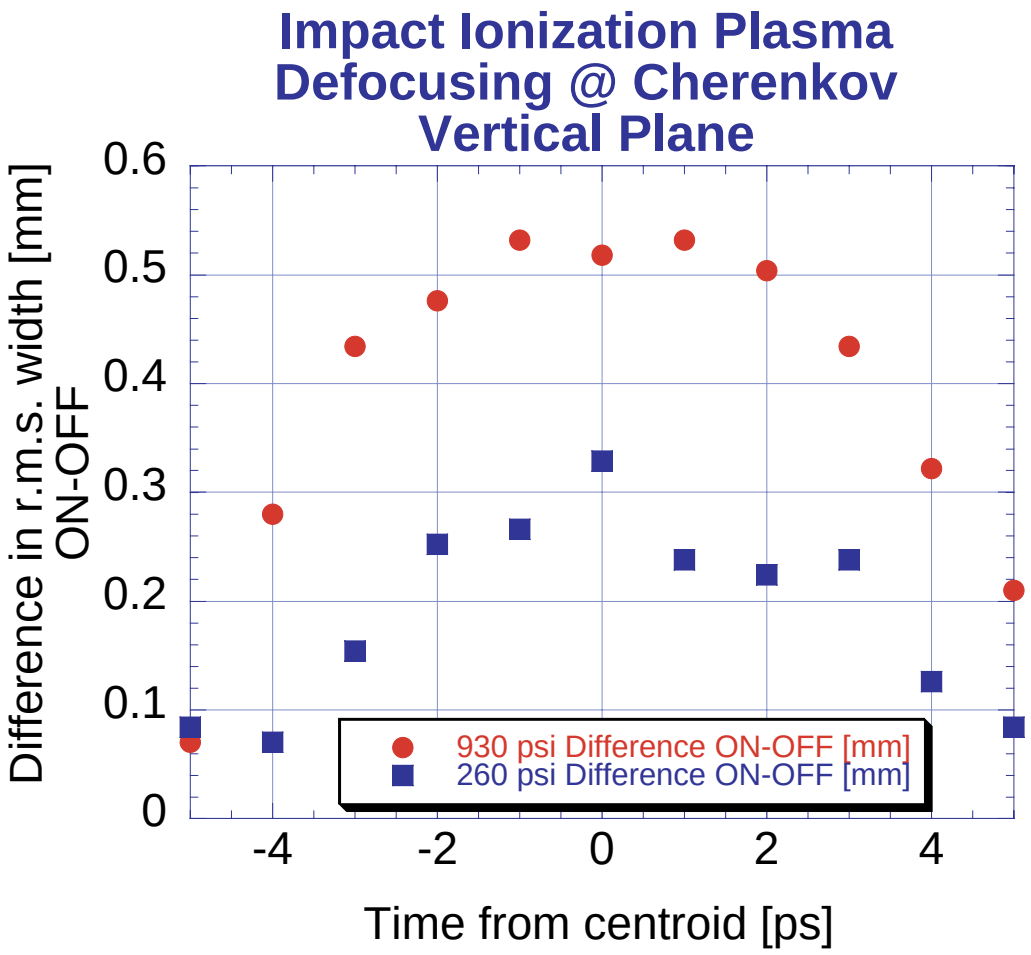

Figure 5: Streak camera diagnostics of plasma focusing longitudinal dynamics.

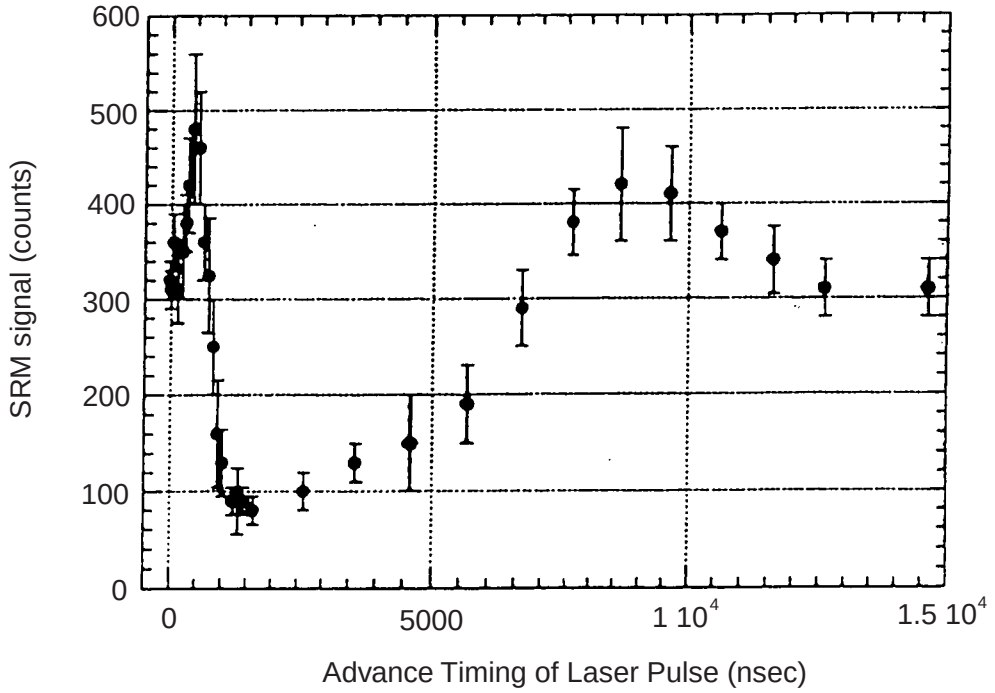

Figure 6: Synchrotron radiation monitor signal (without background subtraction) as a function of the advanced laser ionization timing with respect to beam arrival.